Increased ^{99m}Tc-Sestamibi Accumulation in Normal Liver and Drug-resistant Tumors after the Administration of the Glycoprotein Inhibitor, XR9576

Manish Agrawal, Jame Abraham, Frank M. Balis, Maureen Edgerly, Wilfred D. Stein, Susan Bates, Tito Fojo,[1] and Clara C. Chen

Center for Cancer Research, National Cancer Institute, Bethesda, Maryland 20892 [M. A., F. M. B., M. E., S. B., T. F.]; Mary Babb Cancer Center, West Virginia University, Charleston, West Virginia [J. A.]; Silberman Institute of Life Sciences, Hebrew University, Jerusalem, Israel [W. D. S.]; and Department of Nuclear Medicine, Warren G. Magnuson Clinical Center, National Institutes of Health, Bethesda, Maryland 20892 [C. C. C.]

ABSTRACT

^{99m}Tc-sestamibi, a substrate of the multidrug transporter P-glycoprotein (Pgp), has been used as a functional imaging agent for the multidrug resistance-1 (MDR1) phenotype. *In vitro*, retention of ^{99m}Tc-sestamibi by cells that overexpress Pgp can be enhanced by the addition of Pgp inhibitors. XR9576 (Tariquidar) is a potent and selective noncompetitive inhibitor of Pgp that is active at 25–80 nM. A Phase I trial of XR9576 in combination with vinorelbine (Navelbine) was conducted in 26 patients with metastatic cancers. A ^{99m}Tc-sestamibi scan was obtained at baseline followed 48–96 h later by a second scan 1–3 h after the administration of XR9576. Time activity curves and areas under the curves (AUCs) were obtained for tumor, liver, lung, and heart, and tissue:heart AUC ratios were calculated. XR9576 enhanced ^{99m}Tc-sestamibi accumulation and retention in the liver of all but two patients with a mean change of +128%. Furthermore, in 13 of 17 patients with tumor masses visible by ^{99m}Tc-sestamibi, the tumor:heart ^{99m}Tc-sestamibi $AUC_{0-3\ h}$ increased after the administration of XR9576, with increases of 36–263% seen in 8 patients. We conclude that *in vivo* administration of XR9576 inhibits ^{99m}Tc-sestamibi efflux in both the normal liver and in drug resistant tumors. This study provides convincing evidence of the existence of XR9576-inhibitable ^{99m}Tc-sestamibi efflux in a large fraction of drug resistant tumors. One can predict that efflux of Pgp substrates also occurs in these tumors. XR9576 provides an efficient way to inhibit this efflux and offers the potential to increase drug exposure in human cancer.

INTRODUCTION

Drug resistance is a major impediment to chemotherapy in many human cancers. Pgp[2], a 170-kDa membrane glycoprotein, encoded by the *MDR-1* gene, is the most intensively studied mechanism of drug resistance. Pgp is an energy-dependent efflux pump that lowers the intracellular concentrations of a variety of chemotherapeutic agents, primarily natural products (1–3). Expression of the *MDR-1* gene at levels found in many clinical tumor samples can confer multidrug resistance *in vitro*, suggesting that *MDR*-1/Pgp-mediated drug resistance is clinically relevant.

The anthranilic acid derivative, Tariquidar (XR9576), is a potent and selective Pgp inhibitor that is being developed clinically for the treatment of multidrug-resistant tumors. At concentrations of 25–80 nM, XR9576 can restore the sensitivity of many multidrug-resistant human tumor cell lines to the anthracyclines, *Vinca* alkaloids, taxanes, and epipodophyllotoxins by inhibiting Pgp-mediated drug efflux (4, 5). The duration of action of XR9576 is superior to other inhibitors tested, persisting for at least 22 h after removal of drug from the culture medium. XR9576 uptake into cells is independent of Pgp expression, and the Pgp transport substrates vinblastine and paclitaxel only partially displaced the binding of XR9576 to Pgp. These data suggest that XR9576 is not a transport substrate of Pgp and that the XR9576-mediated inhibition of Pgp transport is noncompetitive.

First generation Pgp inhibitors such as verapamil and cyclosporine had potent pharmacological effects in addition to their ability to inhibit Pgp, and as a result, the dose of these agents was limited by toxicity. Third generation Pgp inhibitors such as XR9576 have been developed to specifically target Pgp and these agents appear to have minimal toxic effects, which are not dose limiting. The optimal dose of third generation Pgp inhibitors will be best assessed with *in vivo* assays that measure a drug's ability to inhibit its target, Pgp, in tumor tissue or in a surrogate tissue. The recognition that ^{99m}Tc-sestamibi, a radionuclide imaging agent marketed for evaluation of cardiac function and for breast imaging, is a Pgp substrate led to its development as an *in vivo* imaging agent for assessment of Pgp inhibition (6, 7).

In this study, we describe the use of ^{99m}Tc-sestamibi imaging of the normal liver and tumors before and after the administration of XR9576 to assess the effect of XR9576 on

Received 6/26/02; revised 9/24/02; accepted 10/1/02.
The costs of publication of this article were defrayed in part by the payment of page charges. This article must therefore be hereby marked *advertisement* in accordance with 18 U.S.C. Section 1734 solely to indicate this fact.

[1] To whom requests for reprints should be addressed, at Center for Cancer Research, Building 10, Room 12N226, 9000 Rockville Pike, Bethesda, MD 20892. Phone: (301) 402-1357; Fax: (301) 402-1608; E-mail: tfojo@helix.nih.gov.

[2] The abbreviations used are: Pgp, P-glycoprotein; TAC, time activity curve; AUC, area under the curve; MDR1, multidrug resistance 1.

Pgp-mediated efflux of this targeted imaging agent. ^{99m}Tc-sestamibi scans showed enhanced retention of the tracer in liver and tumor, suggesting that Pgp-mediated drug efflux occurs in drug resistant tumors and can be modulated by nontoxic doses of XR9576.

PATIENTS AND METHODS

Patients. Twenty-six patients with metastatic cancer were enrolled in a Phase I study combining bolus vinorelbine (Navelbine) administered on a day 1, day 8 schedule with the Pgp antagonist XR9576. All patients consented to undergo two ^{99m}Tc-sestamibi scans. Twenty-five patients had two ^{99m}Tc-sestamibi scans and received protocol therapy; 1 patient, found to have brain metastases after enrollment, was removed from study and received radiation therapy. Patients initially had a baseline (pretreatment) ^{99m}Tc-sestamibi scan. Forty-eight to 96 h later, a 150-mg dose of XR9576 alone was administered i.v., followed by a second ^{99m}Tc-sestamibi scan 1–3 h later. In subsequent cycles, patients received a 150-mg i.v. dose of XR9576 administered over 30 min, beginning 60 min prior to the start of vinorelbine (Navelbine) on days 1 and 8 of a 4-week cycle.

Imaging. Anterior and posterior images were acquired using low-energy/high resolution collimators and a 20% window centered over the 140-keV photopeak of ^{99m}Tc. Large field of view, dual-headed cameras were used (ADAC Laboratories, Milpitas, CA). The same camera was used for both studies in all but 1 patient in whom the camera used at baseline malfunctioned.

Patients were positioned under the camera such that known metastatic lesions were in the field of view with the heart and liver also included whenever possible. Immediately after a bolus administration of 20 mCi of ^{99m}Tc-sestamibi, 30 1-min sequential images were acquired. These were followed by 5-min spot images that were repeated at ~1, 2, and 3 h after the administration of ^{99m}Tc-sestamibi. A conventional whole body scan was also performed after the initial 30-min images.

Image Analysis. Tumor visualization was determined by the nuclear medicine physician without knowledge of the results of other imaging procedures. In patients with tumor masses visualized by ^{99m}Tc-sestamibi, one or more lesions were chosen for analysis. These were lesions that were visualized best and had the least overlap with other normal structures that took up ^{99m}Tc-sestamibi. Using either anterior or posterior images, regions of interest were drawn over the metastatic lesions, normal liver, heart muscle, and lung when possible, and TACs were generated. Curves were background, decay, and dose corrected.

Using the corrected TACs, AUCs were calculated for 0–3 h for each TAC using the linear trapezoidal method. To compare ^{99m}Tc-sestamibi uptake at baseline to that after XR9576 administration, a ratio of the $AUC_{0-3\ h}$ in tissue or tumor to the $AUC_{0-3\ h}$ heart was generated to yield tissue:heart $AUC_{0-3\ h}$. Tissue and tumor AUCs were normalized to the heart muscle AUC to correct for the fact that 3-h images were not always acquired at exactly 180 min after sestamibi injection. Heart muscle was chosen because the heart contains relatively little Pgp and uptake into the heart should not be affected by XR9576 (8, 9). In two cases where the heart was not included in the initial 30 min of scanning, the raw AUC values were used.

The percentage change in liver:heart ^{99m}Tc-Sestamibi $AUC_{0-3\ h}$ shown in Table 1 was calculated using the following formula: [(liver:heart $AUC_{0-3\ h}$ after XR) − (liver:heart $AUC_{0-3\ h}$ before XR)]/(liver:heart $AUC_{0-3\ h}$ before XR) × 100.

RESULTS

Table 1 summarizes the characteristics of the 25 patients that had two ^{99m}Tc-sestamibi scans and received protocol therapy. Patient's ages ranged from 28 to 80 years old (median, 54 years). Eleven were males and 14 were females. Nineteen of 25 patients had disease at more than one site or organ. Seven patients had not received prior chemotherapy, including 6 of 7 patients with renal cell carcinoma, and the patient with carcinoma of the parotid gland. The other 18 patients had received one to seven prior chemotherapy regimens with a median of 3. In these 18 patients, prior chemotherapy regimens included 0–3 Pgp substrates (mean of 2). In an attempt to more accurately reflect the cumulative exposure to Pgp substrates and highlight the extent of prior therapy, the number of doses of Pgp substrates is summarized in Table 1. In these calculations, for example, a patient who received eight cycles of a drug combination consisting of 3 Pgp substrates is shown as having received 24 doses of Pgp substrates. As tabulated in Table 1, these patients had received 0–60 doses of Pgp substrates (median of 30 and mean of 18.3). Although this presentation has limitations and has not been previously validated, it provides some insight into cumulative exposure to Pgp substrates. Those with breast, ovarian, and non-small cell lung cancers had received a median of five prior chemotherapy regimens, including a median of 18.5 doses of Pgp substrates, and were considered drug resistant and eligible for experimental therapy.

Comparison of baseline scans with those performed after the administration of XR9576 showed no obvious visual changes in ^{99m}Tc-sestamibi uptake and retention in normal lung or heart muscle. The lung:heart $AUC_{0-3\ h}$ in the right and left lungs also showed no substantial effect of XR9576 (mean percent change, right lung = +9%; left lung = +2%). For the heart, the mean change in $AUC_{0-3\ h}$ was +2%. In contrast, an increase in retention of ^{99m}Tc-sestamibi was visibly apparent in the liver in almost all patients after XR9576 administration, and this was confirmed by a corresponding increase in liver:heart $AUC_{0-3\ h}$ ratios in 23 of 25 patients. As summarized in Table 1, the mean (range) percentage change from baseline in liver:heart ^{99m}Tc-sestamibi $AUC_{0-3\ h}$ was +128% (range, −14 to +278%). A substantial increase in ^{99m}Tc-sestamibi accumulation was observed in most patients; however, the degree of enhancement of ^{99m}Tc-sestamibi uptake by XR9576 was variable. Although patients received a fixed 150-mg dose of XR9576, there was no correlation between either body surface area or serum levels of XR9576 and the percentage change in liver:heart ^{99m}Tc-sestamibi $AUC_{0-3\ h}$.

In addition to enhanced hepatic accumulation of ^{99m}Tc-sestamibi, tumor visualization was also frequently enhanced after XR9576 (Table 1 and Fig. 1). In 17 of 25 patients, at least one tumor mass was visualized and a ^{99m}Tc-sestamibi $AUC_{0-3\ h}$ calculated. In three of these patients, the tumor was only visu-

Table 1 Patient characteristics and results of ^{99m}Tc-sestamibi imaging

Patient no.	Diagnosis	Age (yr)	Sex	Prior chemotherapy with Pgp substrates[a]		% change liver:heart ^{99m}Tc-sestamibi[b] $AUC_{0-3\,h}$	Lung/chest wall[c]	Liver[c]	Lymph node[c]	Bone/soft tissue[c]
				No. of agents	No. of doses					
1	Clear cell carcinoma	58	M	0	0	111	INC[d]	INC		NV
2	Clear cell carcinoma	36	M	0	0	130	INC		NV	NV
3	Clear cell carcinoma	54	M	0	0	114	INC		INC	INC
4	Clear cell carcinoma	53	M	0	0	75	INC		NV	NV
5	Clear cell carcinoma	63	M	0	0	59	NV		V	INC
6	Clear cell carcinoma	44	M	0	0	198	NV		NOT INC	
7	Papillary carcinoma	63	F	0	0	110			NV	
8	Adrenal cancer	43	F	3	30	229	NV	NV		NV
9	Adrenal cancer	69	F	3	24	222	INC		NV	
10	Adrenal cancer	32	M	3	32	190	INC	INC		NV
11	Adrenal cancer	31	M	3	48	278	INC			NV
12	Breast cancer	80	F	2	11	152	NV	NV	NV	INC
13	Breast cancer	55	F	2	21	56	NOT INC	INC	NOT INC	INC
14	Breast cancer	55	F	3	21	84	NV	NV		
15	Breast cancer	57	F	3	5	218		NV	NV	
16	Breast cancer	52	F	1	6	253				NOT INC
17	Ovarian carcinoma	33	F	2	14	167	NV	NV	NV	NV
18	Ovarian carcinoma	63	F	3	32	174				NV
19	Ovarian carcinoma	44	F	2	11	−14	NV	NOT INC	V	NV
20	Melanoma	66	F	1	3	48				NV
21	NSCLS	49	M	2	9	−3	NOT INC	NV	NV	NV
22	Parotid gland carcinoma	28	F	0	0	67	NOT INC		NV	
23	Basal call carcinoma	48	M	0	0	111	INC			
24	Cervical adenocarcinoma	42	F	1	2	95	INC			NV
25	Ewing's sarcoma	35	M	2	60	122				NV

[a] Prior chemotherapy: each prior Pgp substrate administration was counted as a separate dose. Thus, for example, patient 8 was treated with 3 Pgp substrates on 10 successive cycles ($3 \times 10 = 30$ doses); whereas patient 11 was treated with 3 Pgp substrates for a total of 16 cycles ($3 \times 16 = 48$ doses).

[b] See "Patients and Methods" for calculation used to derive percentage change liver:heart ^{99m}Tc Sestamibi $AUC_{0-3\,h}$.

[c] Four columns on the right indicate sites of disease documented by exam or radiographic studies. Empty box = no metastatic disease at this site or organ.

[d] Results of ^{99m}Tc Sestamibi imaging are summarized as follows: INC, tumor mass visualized in baseline ^{99m}Tc-sestamibi image and tumor:heart $AUC^{0-3\,h}$ increased after XR9576; NOT INC, tumor visualized in baseline ^{99m}Tc-sestamibi image but tumor:heart $AUC_{0-3\,h}$ unchanged or decreased after XR9576; V, tumor visualized but not included in initial field of view, so change in AUC unknown; and NV, ^{99m}Tc-sestamibi imaging did not visualize tumor mass at baseline nor after XR9576 (in patients 7, 8, 14, 15, 17, 18, 20, and 25 tumors not visualized).

alized on the post XR9576 scan. Overall, ^{99m}Tc-sestamibi imaging was able to detect tumor metastases in 17 patients. This included lung metastases in 63% of patients with radiographic documentation of lung lesions, and liver, lymph node, and bone/soft tissue foci in 40, 36, and 28% of patients with known disease in those areas, respectively. In some patients, liver lesions were seen as a photopenic defect.

In 13 of 17 patients with tumor masses visible by ^{99m}Tc-sestamibi, the tumor:heart ^{99m}Tc-sestamibi $AUC_{0-3\,h}$ increased after the administration of XR9576, with increases of 36–263% seen in 8 patients. As can be seen in Fig. 1, the magnitude of the increase in tumor:heart ^{99m}Tc-sestamibi $AUC_{0-3\,h}$ varied among the various lesions in a patient with multiple lesions and among patients. There were two patients with objective responses (patients 3 and 13 in Table 1), and in both of these patients, sestamibi accumulation increased after administration of XR9576. Tumor masses in 5 of 7 patients with renal cell carcinoma and 3 of 4 patients with adrenocortical carcinoma had enhanced uptake of ^{99m}Tc-sestamibi after XR9576. The patients with adrenocortical carcinoma were known to express Pgp as proven on biopsies obtained in prior studies. Because this was a Phase I study, the other patients in this trial did not undergo biopsy to assess the degree of Pgp expression in their tumors. The ^{99m}Tc-sestamibi images at baseline and after administration of XR9576 for 3 patients (patients 3, 5, and 10 in Table 1) are shown in Fig. 2. Increases in ^{99m}Tc-sestamibi accumulations in multiple lung and soft tissue metastases are demonstrated. The thigh metastasis shown in the first example was discovered for the first time on the baseline ^{99m}Tc-sestamibi whole body scan. Fig. 3 demonstrates the effect of XR9576 on ^{99m}Tc-sestamibi clearances in a patient with adrenocortical cancer.

DISCUSSION

This study describes the results of ^{99m}Tc-sestamibi imaging studies in patients enrolled in a Phase I trial of XR9576, a potent and specific Pgp antagonist currently undergoing evaluation as a modulator of multidrug resistance (4, 5). A single 150-mg dose of XR9576 inhibited efflux of ^{99m}Tc-sestamibi from the normal liver and from tumors at various sites in patients with drug resistant cancers. The observation that accumulation of ^{99m}Tc-sestamibi in tumors could be enhanced by XR9576 provides strong evidence of

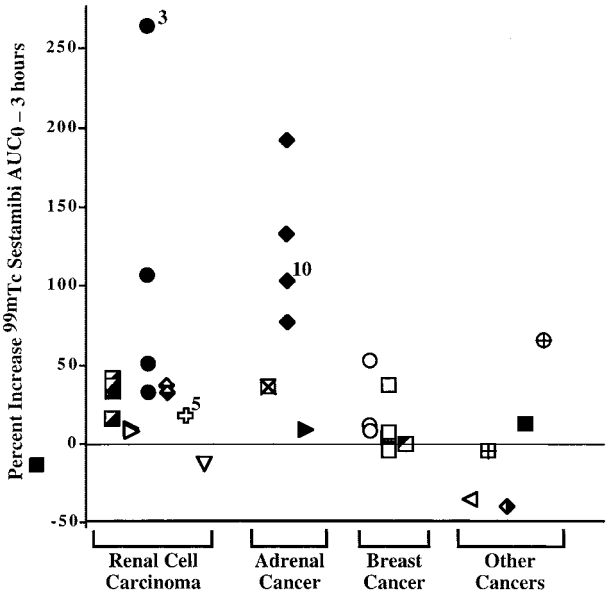

Fig. 1 Changes in ^{99m}Tc-sestamibi accumulations after XR9576 in the 33 tumors visualized and quantified in the 17 patients with visualized tumors categorized by tumor type. Each patient is represented by a different symbol. One to five lesions were quantified in each patient, and these are shown as individual data points, but all lesions from the same patient have the same symbol. The two data points identified as 5 and 10 represent lesions from patients 5 and 10. Images from these patients are shown in Fig. 2. The "Other Cancers" group includes from left to right: ovarian carcinoma; non-small cell lung cancer; parotid gland carcinoma; basal cell carcinoma; and cervical adenocarcinoma.

the expression of the Pgp drug efflux pump in patient's tumors. Previous Pgp antagonists have been hampered by either a lack of potency, the occurrence of dose-limiting side effects, or the need to reduce the dose of chemotherapy because of pharmacokinetic drug interactions (10–13). Because XR9576 and other third generation Pgp blockers appear to be more potent and selective Pgp inhibitors, it should now be possible to properly test the value of blocking Pgp clinically. We would note that in the present study the addition of XR9576 had no effect on vinorelbine pharmacokinetics.[3]

For relatively nontoxic agents such as XR9576, the optimal dose would best be defined using a therapeutic end point rather than toxicity (maximum-tolerated dose), and a variety of *in vivo* and *ex vivo* assays to measure Pgp function and inhibition have been developed (5, 6, 14, 15). ^{99m}Tc-sestamibi imaging has been used to evaluate the efficacy of Pgp inhibitors (16–19), and other studies have correlated ^{99m}Tc-sestamibi imaging with either Pgp expression or clinical response. In breast cancer, several studies have correlated retention of ^{99m}Tc-sestamibi with the levels of Pgp quantified by ^{125}I-labeled MRK-16 binding or more traditional immunohistochemical methods (20–24). Trials evaluating primary and locally advanced breast cancer have demonstrated a correlation between Pgp expression and ^{99m}Tc-sestamibi retention. In addition, several groups have reported that tumors that do not visualize with ^{99m}Tc-sestamibi frequently do not respond to chemotherapy (25–30).

As previously shown for other antagonists, a marked effect was observed on ^{99m}Tc-sestamibi accumulation in the normal liver, most likely reflecting inhibition of Pgp-mediated biliary excretion (16–19, 31). In the absence of XR9576 (baseline studies), ^{99m}Tc-sestamibi is rapidly taken up and then excreted from the liver; and after a period of efflux, ^{99m}Tc-sestamibi levels in the liver are generally well below levels in the heart, which contains relatively little Pgp (32). In contrast, after the administration of XR9576, ^{99m}Tc-sestamibi accumulates in the liver and is retained there. The efflux of ^{99m}Tc-sestamibi is the phase that is markedly affected by XR9576. It is clear that an XR9576-inhibitable efflux system, presumably Pgp, pumps ^{99m}Tc-sestamibi out of the liver. However, close examination revealed that in 13 of 25 patients, the initial rate of liver uptake of ^{99m}Tc-sestamibi in the baseline studies was faster than after the administration of XR9576. This suggests that an XR9576-inhibitable system may also be involved in the uptake of ^{99m}Tc-sestamibi in the liver, raising the possibility that Pgp is also present and active at the blood/liver interface and mediates the accumulation of ^{99m}Tc-sestamibi in the liver. Although unlikely, it should be noted that one cannot rule out alterations in hepatic blood flow after administration of XR9576 as an alternative explanation. More importantly, enhanced ^{99m}Tc-sestamibi accumulations were seen in tumors in a majority of patients. The rapid efflux of ^{99m}Tc-sestamibi from tumors at baseline was blocked after the administration of XR9576, likely representing blockage of Pgp-mediated efflux. The gradual decline of ^{99m}Tc-sestamibi activity seen after the administration of XR9576 may represent non-Pgp mediated efflux, as sestamibi is known to be effluxed by a second ABC transporter, the multidrug resistance-associated protein, which is widely expressed and not blocked by XR9576 (33, 34). Our results raise two questions: (*a*) how sensitive is ^{99m}Tc-sestamibi imaging to Pgp expression within tumors and (*b*) is the magnitude of the enhancement of accumulation of ^{99m}Tc-sestamibi by a Pgp blocker significant? Although this Phase I study cannot provide an accurate estimate of sensitivity, some tentative conclusions can be reached. The accumulated data suggests that lung lesions are most likely to be successfully visualized. In this study, pulmonary metastases were detected by ^{99m}Tc-sestamibi in 63% of patients with known lung metastases. Larger lesions are not necessarily easier to image as demonstrated by a patient with adrenocortical cancer who had too numerous to count lung metastases, many of which were visualized only after the administration of XR9576, whereas in other patients, larger metastases were not seen. ^{99m}Tc-sestamibi was less successful in visualizing liver metastases, which were often seen as photopenic defects in the scans. This is likely because of the avid uptake of ^{99m}Tc-sestamibi by normal liver. Finally, lymph node and bone or soft tissue metastases were detected with a sensitivity of ~28–40%. Although some of these were ideally located in peripheral sites, overlapping sestamibi activity from the heart and the gastrointestinal tract often obscured others in the mediastinum and retroperitoneum. Attenuation by overlapping structures also undoubtedly contributed to the failure of many deep lesions to visualize with sestamibi. Also, because only one region could be chosen for the early 0–30-min images, lesions

[3] J. Abraham *et al.*, manuscript in preparation.

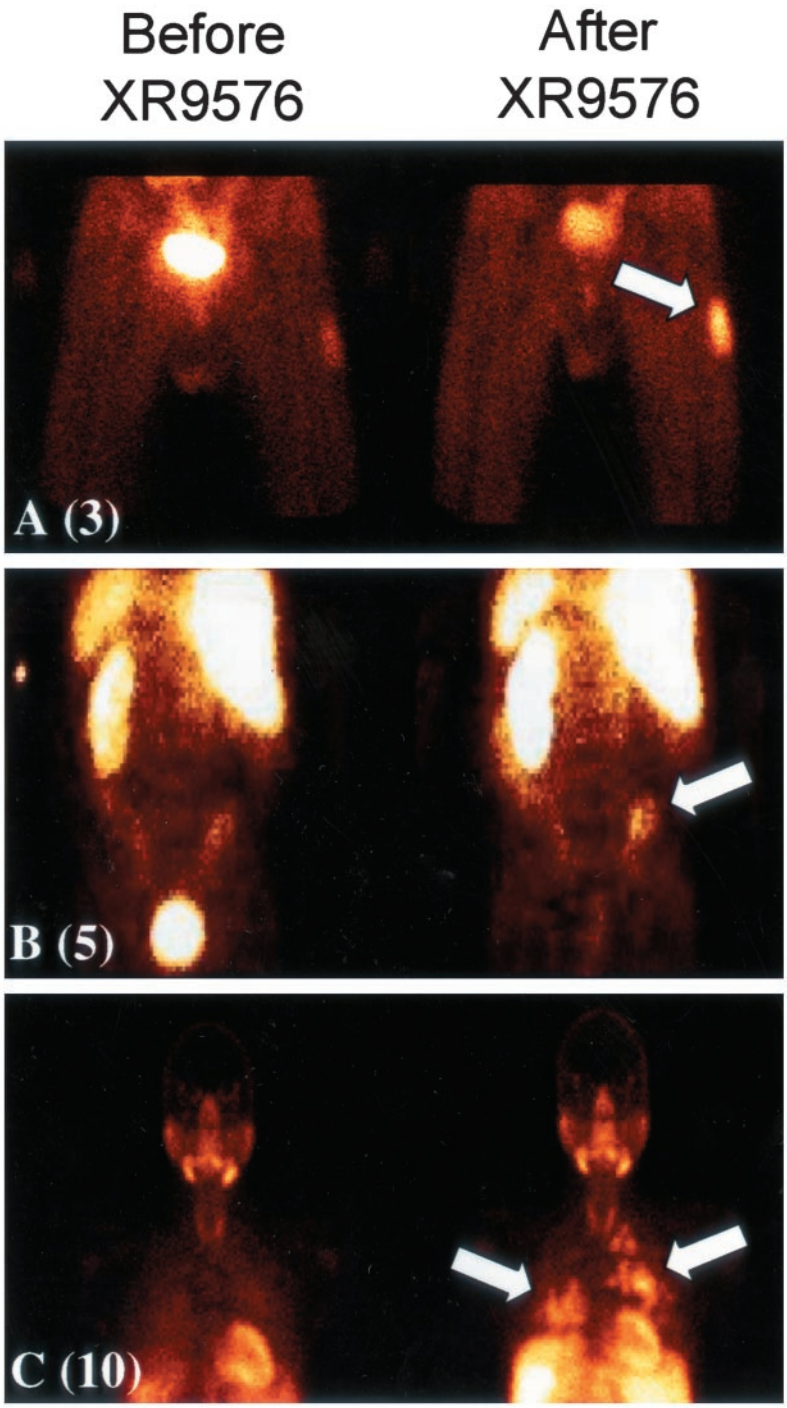

Fig. 2 ^{99m}Tc-sestamibi images at baseline and after administration of XR95767 for patients 3, 5, and 10. Patient numbers are shown in parentheses. *A, arrow* identifies a left thigh mass that had gone undetected until the whole body ^{99m}Tc-sestamibi scan was performed (patient 3, renal cell carcinoma, 263% increase in tumor:heart $AUC_{0-3\,h}$ ratio). *B, arrow* indicates a soft tissue mass invading the iliac bone (patient 5, renal cell carcinoma, 18% increase in tumor:heart $AUC_{0-3\,h}$ ratio). *C, arrows* indicate numerous bilateral lung metastases that are all more readily visualized after the administration of XR9576 (patient 10, adrenocortical carcinoma, 76–191% increase in tumor:heart $AUC_{0-3\,h}$ ratios).

elsewhere in the body with rapid washout of sestamibi were likely missed by the whole body scan performed 30 min after the administration of ^{99m}Tc-sestamibi. Thus, these sensitivities are likely to be underestimates.

As for the significance of the magnitude of the changes in uptake of ^{99m}Tc-sestamibi after XR9576, several facts must be considered. The percentage increases in AUCs are for a 3-h period and thus represent an underestimation of the total increase. More importantly, however, is the fact that the results are based on planar imaging. Regions of interest drawn on planar images include all of the tissue between the tumor and the camera detector, as well as the tissue located behind the tumor in that plane. The inclusion of activity from these overlapping areas diminishes the magnitude of the changes in the tumor. Better results are expected in the future with the development of positron emission tomography using ^{94m}Tc-sestamibi scanning, which will allow for true quantitation.

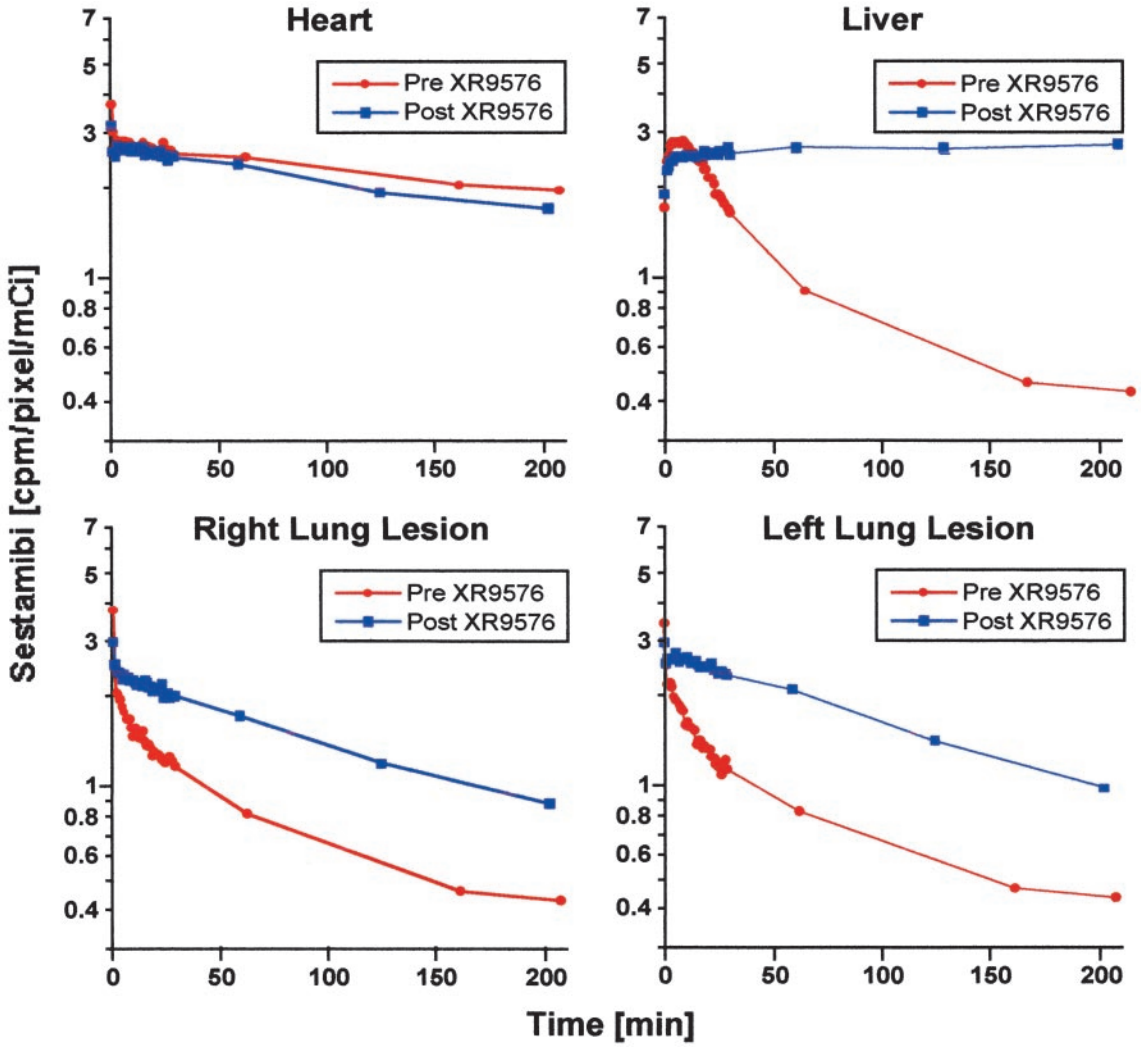

Fig. 3 Effect of XR9576 on ^{99m}Tc-sestamibi disposition in normal heart and liver and two pulmonary metastases in a patient with adrenocortical carcinoma (patient 10). Administration of XR9576 has little effect on ^{99m}Tc-sestamibi accumulation in the heart but results in marked delay in hepatic clearance. The rapid decline in ^{99m}Tc-sestamibi levels in the tumors seen in the baseline scan is partially blocked by the administration of XR9576.

In summary, we report the evaluation of the ability of XR9576 to affect ^{99m}Tc-sestamibi accumulation by various tissues and tumors. As has been previously reported with other Pgp antagonists, a marked effect was observed on the accumulation of ^{99m}Tc-sestamibi in the liver of patients after the administration of XR9576. More importantly, the increases observed in tumors after the administration of XR9576 compare very favorably with those reported with previous Pgp antagonists, suggesting XR9576 might be a more potent antagonist than its predecessors (35). The demonstration that ^{99m}Tc-sestamibi accumulation can be increased by XR9576 provides evidence of the existence of inhibitable ^{99m}Tc-sestamibi efflux and functioning Pgp in these drug-resistant tumors.

Note added in proof:

XR9576 has been assigned the international nonproprietary name, Tariquidar.

REFERENCES

1. Juliano, R. L., and Ling, V. A surface glycoprotein modulating drug permeability in Chinese hamster ovary cell mutants. Biochim. Biophys. Acta, *455:* 152–162, 1976.

2. Fojo, A., Akiyama, S., Gottesman, M. M., and Pastan, I. Reduced drug accumulation in multiply drug-resistant human KB carcinoma cell lines. Cancer Res., *45:* 3002–3007, 1985.

3. Beck, W. T., Mueller, T. J., and Tanzer, L. R. Altered surface membrane glycoproteins in Vinca alkaloid-resistant human leukemic lymphoblasts. Cancer Res., *39:* 2070–2076, 1979.

4. Mistry, P., Stewart, A. J., Dangerfield, W., Okiji, S., Liddle, C., Bootle, D., Plumb, J. A., Templeton, D., and Charlton, P. *In vitro* and *in vivo* reversal of P-glycoprotein-mediated multidrug resistance by a novel potent modulator, XR9576. Cancer Res., *61:* 749–758, 2001.

5. Martin, C., Berridge, G., Mistry, P., Higgins, C., Charlton, P., and Callaghan, R. The molecular interaction of the high affinity reversal agent XR9576 with P-glycoprotein. Br. J. Pharmacol., *28:* 403–411, 1999.

6. Piwnica-Worms, D., Chiu, M. L., Budding, M., Kronauge, J. F., Kramer, R. A., and Croop, J. M. Functional imaging of multidrug-

resistant P-glycoprotein with an organotechnetium complex. Cancer Res., *53:* 977–984, 1993.

7. Rao, V. V., Chiu, M. L., Kronauge, J. F., and Piwnica-Worms, D. Expression of recombinant human multidrug resistance P-glycoprotein in insect cells confers decreased accumulation of technetium-99m-sestamibi. J. Nucl. Med., *35:* 510–515, 1994.

8. Beaulieu, E., Demeule, M., Ghitescu, L., and Beliveau, R. P-glycoprotein is strongly expressed in the luminal membranes of the endothelium of blood vessels in the brain. Biochem. J., *326:* 539–544, 1997.

9. Sugawara, I., Akiyama, S., Scheper, R. J., and Itoyama, S. Lung resistance protein (LRP) expression in human normal tissues in comparison with that of MDR1 and MRP. Cancer Lett., *112:* 23–31, 1997.

10. Ferry, D. R., Traunecker, H., and Kerr, D. J. Clinical trials of P-glycoprotein reversal in solid tumours. Eur. J. Cancer, *32:* 1070–1081, 1996.

11. Fisher, G. A., and Sikic, B. I. Clinical studies with modulators of multidrug resistance. Hematol. Oncol. Clin. N. Am., *9:* 363–382, 1995.

12. Bradshaw, D. M., and Arceci, R. J. Clinical relevance of transmembrane drug efflux as a mechanism of multidrug resistance. J. Clin. Oncol., *16:* 3674–3690, 1998.

13. Fisher, G. A., Lum, B. L., Hausdorff, J., and Sikic, B. I. Pharmacological considerations in the modulation of multidrug resistance. Eur. J. Cancer, *32:* 1082–1088, 1996.

14. Robey, R., Bakke, S., Stein, W., Meadows, B., Litman, T., Patil, S., and Bates, S. Efflux of rhodamine from CD56+ cells as a surrogate marker for reversal of P-glycoprotein-mediated drug efflux by PSC 833. Blood, *93:* 306–314, 1999.

15. Chaudhary, P. M., Mechetner, E. B., and Roninson, I. B. Expression and activity of the multidrug resistance P-glycoprotein in human peripheral blood lymphocytes. Blood, *80:* 2735–2739, 1992.

16. Luker, G. D., Fracasso, P. M., Dobkin, J., and Piwnica-Worms, D. Modulation of the multidrug resistance P-glycoprotein: detection with technetium-99m-sestamibi *in vivo*. J. Nucl. Med., *38:* 369–372, 1997.

17. Bakker, M., van der Graaf, W. T., Piers, D. A., Franssen, E. J., Groen, H. J., Smit, E. F., Kool, W., Hollema, H., Muller, E. A., and deVries, E. G. 99mTc-Sestamibi scanning with SDZ PSC 833 as a functional detection method for resistance modulation in patients with solid tumours. Anticancer Res., *19:* 2349–2353, 1999.

18. Chen, C. C., Meadows, B., Regis, J., Kalafsky, G., Fojo, T., Carrasquillo, J. A., and Bates, S. E. Detection of *in vivo* P-glycoprotein inhibition by PSC 833 using Tc-99m sestamibi. Clin. Cancer Res., *3:* 545–552, 1997.

19. Peck, R. A., Hewett, J., Harding, M. W., Wang, Y. M., Chaturvedi, P. R., Bhatnagar, A., Ziessman, H., Atkins, F., and Hawkins, M. J. Phase I and pharmacokinetic study of the novel MDR1 and MRP1 inhibitor biricodar administered alone and in combination with doxorubicin. J. Clin. Oncol., *19:* 3130–3141, 2001.

20. Del Vecchio, S., Ciarmiello, A., Pace, L., Potena, M. I., Carriero, M. V., Mainolfi, C., Thomas, R., D'Aiuto, G., Tsuruo, T., and Salvatore, M. Fractional retention of technetium-99m-sestamibi as an index of P-glycoprotein expression in untreated breast cancer patients. J. Nucl. Med., *38:* 1348–1351, 1997.

21. Sun, S. S., Hsieh, J. F., Tsai, S. C., Ho, Y. J., Lee, J. K., and Kao, C. H. Expression of mediated P-glycoprotein multidrug resistance related to Tc-99m MIBI scintimammography results. Cancer Lett., *153:* 95–100, 2000.

22. Sun, S. S., Hsieh, J. F., Tsai, S. C., Ho, Y. J., and Kao, C. H. Expression of drug resistance protein related to Tc-99m MIBI breast imaging. Anticancer Res., *20:* 2021–2025, 2000.

23. Ciarmiello, A., Del Vecchio, S., Silvestro, P., Potena, M. I., Carriero, M. V., Thomas, R., Botti, G., D'Aiuto, G., and Salvatore, M. Tumor clearance of technetium 99m-sestamibi as a predictor of response to neoadjuvant chemotherapy for locally advanced breast cancer. J. Clin. Oncol., *16:* 1677–1683, 1998.

24. Vecchio, S. D., Ciarmiello, A., Potena, M. I., Carriero, M. V., Mainolfi, C., Botti, G., Thomas, R., Cerra, M., D'Aiuto, G., Tsuruo, T., and Salvatore, M. *In vivo* detection of multidrug-resistant (MDR1) phenotype by technetium-99m sestamibi scan in untreated breast cancer patients Eur. J. Nucl. Med., *24:* 150–159, 1997.

25. Burak, Z., Ersoy, O., Moretti, J. L., Erinc, R., Ozcan, Z., Dirlik, A., Sabah, D., and Basdemir, G. The role of 99mTc-MIBI scintigraphy in the assessment of MDR1 overexpression in patients with musculoskeletal sarcomas: comparison with therapy response. Eur. J. Nucl. Med., *28:* 1341–1350, 2001.

26. Kao, C. H., Tsai, S. C., Wang, J. J., Ho, Y. J., Ho, S. T., and Changlai, S. P. Evaluation of chemotherapy response using technetium-99M-sestamibi scintigraphy in untreated adult malignant lymphomas and comparison with other prognosis factors: a preliminary report. Int. J. Cancer, *95:* 228–231, 2001.

27. Kao, C. H., Tsai, S. C., Liu, T. J., Ho, Y. J., Wang, J. J., Ho, S. T., and ChangLai, S. P. P-Glycoprotein and multidrug resistance-related protein expressions in relation to technetium-99m methoxyisobutylisonitrile scintimammography findings. Cancer Res., *61:* 1412–1414, 2001.

28. Yamamoto, Y., Nishiyama, Y., Satoh, K., Takashima, H., Ohkawa, M., Fujita, J., Kishi, T., Matsuno, S., and Tanabe, M. Comparative study of technetium-99m-sestamibi and thallium-201 SPECT in predicting chemotherapeutic response in small cell lung cancer. J. Nucl. Med., *39:* 1626–1629, 1998.

29. Nishiyama, Y., Yamamoto, Y., Satoh, K., Ohkawa, M., Kameyama, K., Hayashi, E., Fujita, J., and Tanabe, M. Comparative study of Tc-99m MIBI and TI-201 SPECT in predicting chemotherapeutic response in non-small-cell lung cancer. Clin. Nucl. Med., *25:* 364–369, 2000.

30. Komori, T., Narabayashi, I., Matsui, R., Sueyoshi, K., Aratani, T., and Utsunomiya, K. Technetium-99m MIBI single photon emission computed tomography as an indicator of prognosis for patients with lung cancer-preliminary report. Ann. Nucl. Med., *14:* 415–420, 2000.

31. Kabasakal, L., Halac, M., Nisli, C., Oguz, O., Onsel, C., Civi, G., and Uslu, I. The effect of P-glycoprotein function inhibition with cyclosporine A on the biodistribution of Tc-99m sestamibi. Clin. Nucl. Med., *25:* 20–23, 2000.

32. Fojo, A. T., Ueda, K., Slamon, D. J., Poplack, D. G., Gottesman, M. M., and Pastan, I. Expression of a multidrug-resistance gene in human tumors and tissues. Proc. Natl. Acad. Sci. USA, *84:* 265–269, 1987.

33. Hendrikse, N. H., Franssen, E. J., van der Graaf, W. T., Meijer, C., Piers, D. A., Vaalburg, W., and deVries, E. G. 99mTc-sestamibi is a substrate for P-glycoprotein and the multidrug resistance-associated protein. Br. J. Cancer, *77:* 353–358, 1998.

34. Utsunomiya, K., Ballinger, J. R., Piquette-Miller, M., Rauth, A. M., Tang, W., Su, Z. F., and Ichise, M. Comparison of the accumulation and efflux kinetics of technetium-99m sestamibi and technetium-99m tetrofosmin in an MRP-expressing tumour cell line. Eur. J. Nucl. Med., *27:* 1786–1792, 2000.

35. Stewart, A., Steiner, J., Mellows, G., Laguda, B., Norris, D., and Bevan, P. Phase I trial of XR9576 in healthy volunteers demonstrates modulation of P-glycoprotein in CD56+ lymphocytes after oral and intravenous administration. Clin. Cancer Res., *6:* 4186–4191, 2000.

Clinical Cancer Research

Increased ^{99m}Tc-Sestamibi Accumulation in Normal Liver and Drug-resistant Tumors after the Administration of the Glycoprotein Inhibitor, XR9576

Manish Agrawal, Jame Abraham, Frank M. Balis, et al.

Clin Cancer Res 2003;9:650-656.